A DISCRETIZATION-CONSISTENT LENGTH SCALE DEFINITION FOR LARGE-EDDY SIMULATIONS OF COMPLEX FLOWS

F.X.Trias[1], **J.Ruano**[1], **A.Duben**[2], **A.Gorobets**[2]
[1]Heat and Mass Transfer Technological Center, Technical University of Catalonia
c/Colom 11, 08222 Terrassa (Barcelona), Spain
[2]Keldysh Institute of Applied Mathematics, 4A, Miusskaya Sq., Moscow 125047, Russia
francesc.xavier.trias@upc.edu

INTRODUCTION

Large-eddy simulation (LES) equations are obtained by applying a spatial, commutative filtering operation with filter length δ, to the Navier–Stokes equations

$$\partial_t \overline{\boldsymbol{u}} + (\overline{\boldsymbol{u}}\cdot\nabla)\,\overline{\boldsymbol{u}} = \nu\nabla^2\overline{\boldsymbol{u}} - \nabla\overline{p} - \nabla\cdot\tau(\overline{\boldsymbol{u}}), \quad \nabla\cdot\overline{\boldsymbol{u}} = 0, \quad (1)$$

where $\overline{\boldsymbol{u}}$ denotes the filtered velocity and $\tau(\overline{\boldsymbol{u}})$ is the subgrid stress (SGS) tensor, which accounts for the effect of the unresolved turbulent motions. The SGS tensor is given by $\tau(\overline{\boldsymbol{u}}) \approx \overline{\boldsymbol{u}\otimes\boldsymbol{u}} - \overline{\boldsymbol{u}}\otimes\overline{\boldsymbol{u}}$ and must be modeled to close the filtered equations. Due to its simplicity and robustness, the eddy-viscosity assumption remains the most widely used closure. Within this framework, the SGS stresses are approximated as

$$\tau(\overline{\boldsymbol{u}}) \approx -2\nu_t S(\overline{\boldsymbol{u}}), \quad (2)$$

where $S(\overline{\boldsymbol{u}})$ is the rate-of-strain tensor and ν_t denotes the eddy-viscosity. The latter is commonly expressed as

$$\nu_t = (C_m\delta)^2 D_m(\overline{\boldsymbol{u}}). \quad (3)$$

In recent decades, most research efforts within the LES community have focused either on the determination of the model constant C_m (*e.g.* through dynamic procedures and their variants) or on the development of improved model operators $D_m(\overline{\boldsymbol{u}})$, such as the WALE, Vreman, QR-model, σ, or the S3PQR model [1]. In contrast, considerably less attention has been devoted to the definition of the subgrid characteristic length, δ, despite its fundamental role in eddy-viscosity closures (see Eq. 3). Due to its simplicity and straightforward applicability to unstructured meshes, the definition originally proposed by Deardorff [2], namely the cube root of the cell volume (see Eq. 5), remains the most widely adopted choice in practical computations although it may lead to inaccurate results [3, 4, 5].

Alternative definitions of the subgrid characteristic length δ are summarized and classified in Table 1 according to a set of desirable properties for a consistent definition of δ. Based on property **P3**, these definitions can be grouped into two main categories: (i) formulations in which δ depends solely on the geometrical properties of the mesh, and (ii) formulations in which δ also depends on the local flow topology. The latter class incorporates information from the gradient of the resolved velocity field, $\mathsf{G}\equiv\nabla\overline{\boldsymbol{u}}$, whereas the local mesh geometry, for a Cartesian grid, is characterized by

$$\Delta \equiv \mathrm{diag}(\Delta x, \Delta y, \Delta z). \quad (4)$$

Without loss of generality, hereafter we assume that $\Delta x \leq \Delta y \leq \Delta z$. The first seven definitions listed in Table 1 are

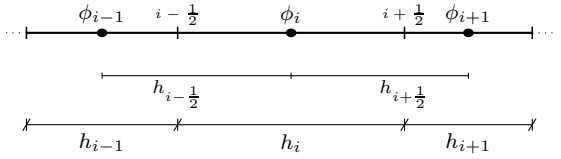

Figure 1: One-dimensional mesh

$$\delta_{\mathrm{vol}} = (\Delta x\Delta y\Delta z)^{1/3}, \quad \delta_{\mathrm{Sco}} = f(a_1,a_2)\delta_{\mathrm{vol}}, \quad (5)$$

$$\delta_{\max} = \max(\Delta x, \Delta y, \Delta z), \quad (6)$$

$$\delta_{\boldsymbol{\omega}} = \sqrt{\frac{\omega_x^2\Delta y\Delta z + \omega_y^2\Delta x\Delta z + \omega_z^2\Delta x\Delta y}{|\boldsymbol{\omega}|^2}}, \quad (7)$$

$$\tilde{\delta}_{\boldsymbol{\omega}} = \max_{n,m}\frac{|\boldsymbol{l}_n - \boldsymbol{l}_m|}{\sqrt{3}}, \ \delta_{\mathrm{SLA}} = \tilde{\delta}_{\boldsymbol{\omega}} F_{\mathrm{KH}}(VTM) \quad (8)$$

$$\delta_{\mathrm{lsq}} = \sqrt{(\mathsf{G}_\delta\mathsf{G}_\delta^T : \mathsf{G}\mathsf{G}^T)/(\mathsf{G}\mathsf{G}^T : \mathsf{G}\mathsf{G}^T)}, \quad (9)$$

where $\boldsymbol{\omega} = \nabla\times\boldsymbol{u}$ is the vorticity and $f(a_1,a_2) = \cosh\sqrt{4/27[(\ln a_1)^2 - \ln a_1\ln a_2 + (\ln a_2)^2]}$ was introduced by Scotti [6] as a correction for grid anisotropy. The factor $0 \leq F_{\mathrm{KH}}(VTM) \leq 1$, proposed by Shur *et al.* [7], modifies the definition originally introduced by Mockett *et al.* [8] in the context of Detached Eddy Simulation. Later on, δ_{lsq} was proposed by co-authors of this work [3], where $\mathsf{G}_\delta \equiv \mathsf{G}\Delta$ denotes the velocity-gradient tensor in the computational space. The classification in Table 1 is based on physical, numerical, and practical considerations. The list is completed by the novel definitions δ_{rls} and $\tilde{\delta}_{\mathrm{rls}}$ recently proposed by the authors [5]. Here, we revise the main ideas and extend the analysis for complex geometries and unstructured meshes.

FINITE-VOLUME FILTERING

Let us consider a 1D convection-diffusion equation

$$\frac{\partial\phi}{\partial t} + \frac{\partial(u\phi)}{\partial x} = \frac{\partial}{\partial x}\left(\Gamma\frac{\partial\phi}{\partial x}\right), \quad (10)$$

where $u(x,t)$ denotes the advective velocity and $\phi(x,t)$ a transported scalar. In a FVM, the discrete variables correspond to box-filtered quantities with filter width equal to the local grid spacing h,

$$\overline{\phi}(x) = \frac{1}{h}\int_{x-\frac{h}{2}}^{x+\frac{h}{2}}\phi dx. \quad (11)$$

Notice that the box filtering commutes with differentiation

$$\frac{\partial\overline{\phi}}{\partial x} = \frac{1}{h}\frac{\partial}{\partial x}\int_{x-\frac{h}{2}}^{x+\frac{h}{2}}\phi dx = \frac{1}{h}\int_{x-\frac{h}{2}}^{x+\frac{h}{2}}\frac{\partial\phi}{\partial x}dx = \overline{\frac{\partial\phi}{\partial x}}. \quad (12)$$

	δ_{vol}	δ_{Sco}	$\delta_{\max}$	$\delta_{\boldsymbol{\omega}}$	$\tilde{\delta}_{\boldsymbol{\omega}}$	δ_{SLA}	δ_{lsq}	δ_{rls}	$\tilde{\delta}_{\text{rls}}$
Formula	Eq.(5)	Eq.(5)	Eq.(6)	Eq.(7)	Eq.(8)	Eq.(8)	Eq.(9)	Fig.(2)	Eq.(19)
P1	Yes	Yes	Yes	Yes	Yes	Yes	Yes	Yes	Yes
P2	Yes	Yes	Yes	Yes	Yes	No	Yes	Yes	Yes
P3	No	No	No	Yes	Yes	Yes	Yes	No[c]	Yes
P4	Yes	No	No[a]	No[b]	Yes	Yes	Yes	Yes	Yes
P5	No	No	No	No	No	No	No	Yes	No
P6	+	+	+	+	+ + +	+ + ++	+ + +	+	+ + +
P7	+	+	+	+	++	+ + +	+ + +	+	+ + +

Table 1: Comparison of different definitions of the subgrid characteristic length, δ. The classification is based on a set of physical, numerical, and practical properties: **P1** positivity, locality, and frame invariance; **P2** boundedness (for a Cartesian mesh with $\Delta x \leq \Delta y \leq \Delta z$, $\Delta x \leq \delta \leq \Delta z$); **P3** sensitivity to the local flow field through the velocity gradient G; **P4** applicability to unstructured meshes; **P5** computation of the length scale directly at cell faces; **P6** computational cost; and **P7** memory footprint. [a] Possible with some adaptations, [b] Deck [9] proposed a generalization for unstructured meshes. [c] Although δ_{rls} is computed independently of the local flow field, its effect ultimately depends on it.

Moreover, the second-order approximation of the spatial derivative at the face is equal to the filtered derivative,

$$\left.\frac{\partial \phi}{\partial x}\right|_{i+\frac{1}{2}} \approx \frac{\phi_{i+1}-\phi_i}{h_{i+\frac{1}{2}}} = \frac{1}{h_{i+\frac{1}{2}}}\int_{x_i}^{x_{i+1}} \frac{\partial \phi}{\partial x} dx = \left.\overline{\frac{\partial \phi}{\partial x}}\right|_{i+\frac{1}{2}} \overset{Eq.(12)}{=} \left.\frac{\partial \overline{\phi}}{\partial x}\right|_{i+\frac{1}{2}}. \tag{13}$$

Remark 1 *This indicates that the effective filter width associated with the computation of the face derivative is the distance between adjacent nodes, $h_{i+\frac{1}{2}}$ (see Figure 1).*

Finally, in a FVM, the diffusive term is discretized as

$$\begin{aligned}\left.\frac{\partial}{\partial x}\left(\Gamma\frac{\partial \phi}{\partial x}\right)\right|_i &\approx \frac{1}{h_i}\left(\Gamma\left.\frac{\partial \phi}{\partial x}\right|_{i+\frac{1}{2}} - \Gamma\left.\frac{\partial \phi}{\partial x}\right|_{i-\frac{1}{2}}\right) \\ &= \left.\overline{\frac{\partial}{\partial x}\left(\Gamma\frac{\partial \phi}{\partial x}\right)}\right|_i \\ &\approx \frac{1}{h_i}\left(\Gamma_{i+\frac{1}{2}}\frac{\phi_{i+1}-\phi_i}{h_{i+\frac{1}{2}}} - \Gamma_{i-\frac{1}{2}}\frac{\phi_i-\phi_{i-1}}{h_{i-\frac{1}{2}}}\right) \\ &= \left.\overline{\frac{\partial}{\partial x}\left(\Gamma\overline{\frac{\partial \phi}{\partial x}}\right)}\right|_i. \end{aligned} \tag{14}$$

For spatially varying diffusivity, $\Gamma(x)$, the evaluation of the previous expression can be viewed as filtering the Γ field, *i.e.*

$$\Gamma_{i+\frac{1}{2}} \approx \frac{\Gamma_i+\Gamma_{i+1}}{2} \approx \frac{1}{h_{i+\frac{1}{2}}}\int_{x_i}^{x_{i+1}} \Gamma(x)dx = \overline{\Gamma}_{i+\frac{1}{2}}, \tag{15}$$

where the integral is approximated using the trapezoidal rule. Combining the expressions above yields

$$\begin{aligned}&\left.\frac{\partial}{\partial x}\left(\Gamma\frac{\partial \phi}{\partial x}\right)\right|_i \approx \\ &\frac{1}{h_i}\left(\frac{\Gamma_{i+1}+\Gamma_i}{2}\frac{\phi_{i+1}-\phi_i}{h_{i+\frac{1}{2}}} - \frac{\Gamma_i+\Gamma_{i-1}}{2}\frac{\phi_i-\phi_{i-1}}{h_{i-\frac{1}{2}}}\right) \\ &\qquad = \left.\overline{\frac{\partial}{\partial x}\left(\overline{\Gamma}\overline{\frac{\partial \phi}{\partial x}}\right)}^{FV}\right|_i, \end{aligned} \tag{16}$$

where $\overline{(\cdot)}^{FV}$ is the FVM filtering along the cell i, while the remaining two filters act at the cell faces with characteristic lengths $h_{i+\frac{1}{2}}$ and $h_{i-\frac{1}{2}}$, respectively.

Remark 2 *The above analysis indicates that two distinct filtering operations are involved in the evaluation of the diffusive term: the computation of the face derivative (see Eq. 13) and the cell-to-face interpolation of the diffusivity Γ (see Eq. 15). Both operations are associated with the same characteristic filter length; namely, the distance between the two nodes adjacent to the corresponding face.*

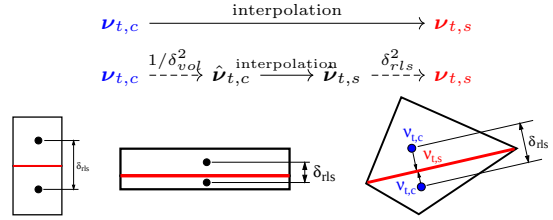

Figure 2: Top: flow chart for the implementation of the δ_{rls}. Dashed lines represent the modifications required respect to the usual flow chart. Bottom: *FLrls* for different types of meshes including an unstructured one on which the above-explained flow chart is visually represented.

Consequently, this suggests that the SGS characteristic length employed in the evaluation of the eddy viscosity, ν_t, at the face $i+\frac{1}{2}$ should naturally be $h_{i+\frac{1}{2}}$ (see Figure 1). This observation constitutes the cornerstone of this work and provides a natural way for extending it to general meshes, including unstructured ones.

A RATIONALE LENGTH SCALE FOR COMPLEX FLOWS

The subgrid characteristic length, δ, appears in a natural way when we consider the calculation of the ν_t at the cell faces. The flowchart shown in Figure 2 shows that it basically consists on firstly computing the $\hat{\boldsymbol{\nu}}_{t,c}$ at the cells without considering any characteristic length, then interpolating this quantity to the faces. Finally, this quantity at the face is re-scaled by the square of the cell distances. Therefore, from an implementation and conceptual point-of-view, the new approach δ_{rls} (rls stands for *r*ational *l*ength *s*cale) is completely different from all previous definitions of δ. Although the required code modifications are minimal (see flowchart in Figure 2), it may be of interest to compute an equivalent length scale that provides the same dissipation. Namely, it can be shown that the local dissipation of the viscous term, with constant viscosity, is

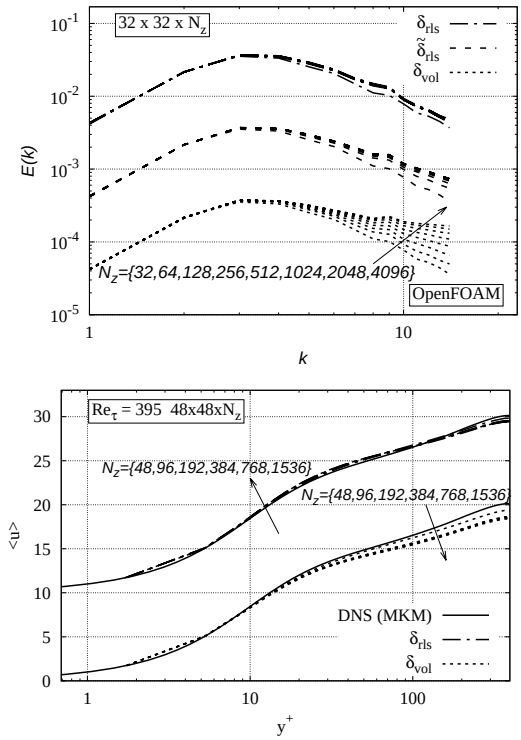

Figure 3: Top: energy spectra for decaying isotropic turbulence (Comte-Bellot and Corrsin [10]). Results obtained with the proposed definitions δ_{rls} and $\tilde{\delta}_{\text{rls}}$ are compared with δ_{vol}. For clarity, the curves corresponding to $\tilde{\delta}_{\text{rls}}$ and δ_{vol} are shifted down one and two decades, respectively. Bottom: mean velocity profile for turbulent channel flow at $Re_\tau = 395$. LES results obtained using δ_{rls} are compared with δ_{vol}, both employing the S3QR model [1].

given by

$$\nu \mathsf{G} : \mathsf{G} = \nu tr(\mathsf{G}\mathsf{G}^T). \tag{17}$$

If we replace ν by ν_t, we can obtain a very accurate estimation of the local dissipation introduced by an eddy-viscosity model. Moreover, in the new approach we need to replace ν_t and G by $\hat{\nu}_t$ and G_δ, respectively, leading to

$$\hat{\nu}_t \mathsf{G}_\delta : \mathsf{G}_\delta = \hat{\nu}_t tr(\mathsf{G}_\delta \mathsf{G}_\delta^T). \tag{18}$$

Then, we can compute an equivalent filter length, $\tilde{\delta}_{\text{rls}}$, that leads to the same local dissipation, *i.e.*

$$\tilde{\delta}_{\text{rls}}^2 \hat{\nu}_t \mathsf{G} : \mathsf{G} = \hat{\nu}_t \mathsf{G}_\delta : \mathsf{G}_\delta \quad \Longrightarrow$$

$$\boxed{\tilde{\delta}_{\text{rls}} = \sqrt{\frac{\mathsf{G}_\delta : \mathsf{G}_\delta}{\mathsf{G} : \mathsf{G}}} = \sqrt{\frac{tr(\mathsf{G}_\delta \mathsf{G}_\delta^T)}{tr(\mathsf{G}\mathsf{G}^T)}}} \tag{19}$$

NUMERICAL RESULTS AND CONCLUSIONS

The proposed discretization-consistent length scale is assessed using LES of decaying isotropic turbulence. As shown in Figure 3 (top), increasing mesh anisotropy leads to a rapid loss of subgrid dissipation when the classical Deardorff length scale is employed, resulting in a strong dependence of the solution on the grid resolution. In contrast, the proposed definitions δ_{rls} and $\tilde{\delta}_{\text{rls}}$ preserve a consistent level of dissipation and exhibit rapid convergence as the mesh is refined. Additional simulations of a turbulent channel flow (see Figure 3, bottom) confirm the improved behavior of the proposed length scale in wall-bounded configurations, particularly on stretched grids.

These results confirm the robustness of the proposed discretization-consistent length scale and its reduced sensitivity to mesh anisotropy. The complete setup for these cases, including the input files and the modifications to the `TurbulenceModel` library required to reproduce the results in OpenFOAM, is publicly available [11]. Comparisons with other numerical codes, as well as results for unstructured grids and more complex flows, will be presented at the conference and discussed in the final paper. The proposed formulation will also be investigated in the context of DES simulations.

ACKNOWLEDGMENTS

F.X.T. and J.R. are supported by SIMEX project (PID2022-142174OB-I00) of the *Ministerio de Ciencia e Innovación* MCIN/AEI/ 10.13039/501100011033 and the European Union Next GenerationEU. Calculations were carried out on the MareNostrum 5-GPP supercomputer at BSC. We thankfully acknowledge these institutions.

REFERENCES

[1] F. X. Trias, D. Folch, A. Gorobets, and A. Oliva. Building proper invariants for eddy-viscosity subgrid-scale models. *Physics of Fluids*, 27(6):065103, 2015.

[2] J. W. Deardorff. Numerical study of three-dimensional turbulent channel flow at large Reynolds numbers. *Journal of Fluid Mechanics*, 41:453–480, 1970.

[3] F. X. Trias, A. Gorobets, M. H. Silvis, R. W. C. P. Verstappen, and A. Oliva. A new subgrid characteristic length for turbulence simulations on anisotropic grids. *Physics of Fluids*, 26:115109, 2017.

[4] J. Schumann, S. Toosi, and J. Larsson. Assessment of grid anisotropy effects on large-eddy-simulation models with different length scales. *AIAA Journal*, 58(10):4522 – 4533, 2020.

[5] F. X. Trias, J. Ruano, A. Duben, and A. Gorobets. A rational length scale for large-eddy simulation of turbulence on anisotropic grids. *Physics of Fluids*, 37(8):085239, 2025.

[6] A. Scotti, C. Meneveau, and D. K. Lilly. Generalized Smagorinsky model for anisotropic grids. *Physics of Fluids A*, 5(9):2306–2308, 1993.

[7] M. L. Shur, P. R. Spalart, M. K. Strelets, and A. K. Travin. An Enhanced Version of DES with Rapid Transition from RANS to LES in Separated Flows. *Flow, Turbulence and Combustion*, 95:709–737, 2015.

[8] C. Mockett, M. Fuchs, A. Garbaruk, M. Shur, P. Spalart, M. Strelets, F. Thiele, and A. Travin. Two Non-zonal Approaches to Accelerate RANS to LES Transition of Free Shear Layers in DES. In Sharath Girimaji, Werner Haase, Shia-Hui Peng, and Dieter Schwamborn, editors, *Progress in Hybrid RANS-LES Modelling*, volume 130 of *Notes on Numerical Fluid Mechanics and Multidisciplinary Design*, pages 187–201. Springer International Publishing, 2015.

[9] S. Deck. Recent improvements in the Zonal Detached Eddy Simulation (ZDES) formulation. *Theoretical and Computational Fluid Dynamics*, 26(6):523–550, 2012.

[10] G. Comte-Bellot and S. Corrsin. Simple Eulerian time correlation of full- and narrow-band velocity signals in grid-generated, isotropic turbulence. *Journal of Fluid Mechanics*, 48:273–337, 1971.

[11] J. Ruano, 2025. `https://github.com/jruanoperez/DHIT`.